Article

Not peer-reviewed version

Evaluation of ^{177}Lu-PSMA-617 Based Targeted Radioligand Therapy with X-Ray Stimulated PSMA Relocation in the *PiggyBac* Reporter Gene Engineered Orthotopic Prostate Tumor Model

Yen-Ta Chen †, Ke-Xin Huang †, Chun-Yi Wu, Yi-Jang Lee *

Posted Date: 31 March 2026

doi: 10.20944/preprints202603.2479.v1

Keywords: slow-growing prostate cancer; *PiggyBac* transposon system; reporter gene imaging; prostate-specific membrane antigen; orthotopic tumor model

 doi:10.20944/preprints202603.2479.v1

Article

Evaluation of ^{177}Lu-PSMA-617 Based Targeted Radioligand Therapy with X-Ray Stimulated PSMA Relocation in the *PiggyBac* Reporter Gene Engineered Orthotopic Prostate Tumor Model

Running Title: Imaging of Combined EBRT and PSMA-RLT in Prostate Cancer Model

Yen-Ta Chen [1,†], Ke-Xin Huang [2,†], Chun-Yi Wu [2] and Yi-Jang Lee [2,3,*]

[1] Division of Urology, Department of Surgery, Kaohsiung Chang Gung Memorial Hospital, Chang Gung University College of Medicine, Kaohsiung 833401, Taiwan

[2] Department of Biomedical Imaging and Radiological Sciences, National Yang-Ming Chiao Tung University, Taipei, 112 Taiwan

[3] Cancer and Immunology Research Center, National Yang Ming Chiao Tung University, Taipei Branch, Taipei 112, Taiwan

* Correspondence: yjlee2@nycu.edu.tw; Tel: 886-2-28267189; Fax: 886-2-28201095

† These authors contributed equally.

Abstract

Because human prostate cancer (PCa) grows slowly, establishing PCa tumor models is often time-consuming and unpredictable, limiting the efficiency of preclinical theranostic development. To address this, we used a non-viral *PiggyBac* transposon system to introduce triple reporter genes into PSMA-expressing C4-2 cells, generating orthotopic and subcutaneous xenograft models that allow noninvasive, real-time monitoring of PCa progression and treatment response. Reporter-engineered C4-2 3R cells were produced by co-transfecting constructs encoding the reporter cassette and PB transposase, followed by enrichment using fluorescence microscopy and FACS, and implanted orthotopically or subcutaneously into mice. Tumor growth and response to a single 2 Gy X-ray dose followed by 14.8 MBq ^{177}Lu-PSMA-617, or to each monotherapy, were monitored weekly using IVIS imaging and confirmed by tumor dissection and H&E staining; PSMA expression was assessed by western blot and ^{18}F-PSMA-1007 PET/CT. C4-2 3R cells successfully expressed mRFP, luc2, and HSV1-tk, generating detectable orthotopic bioluminescence within one week and persisting for at least five weeks, whereas subcutaneous implantation produced only transient luc2 signals with no tumor formation. X-ray exposure did not increase total PSMA levels but induced PSMA relocation to the cell membrane. Combined external beam radiotherapy (EBRT) and ^{177}Lu-PSMA-617 treatment produced the highest ^{18}F-PSMA-1007 uptake and strongest tumor suppression, with minimal residual tumor mass compared to single-treatment or control groups. Overall, the C4-2 3R reporter model enables faster, reliable monitoring of slow-growing PCa tumors and provides an effective platform for evaluating PSMA-targeted therapies with or without the combination of EBRT.

Keywords: slow-growing prostate cancer; *PiggyBac* transposon system; reporter gene imaging; prostate-specific membrane antigen; orthotopic tumor model

Introduction

Prostate cancer (PCa) is the most commonly diagnosed malignancy and a leading cause of cancer-related death among men worldwide. However, PCa is known a slow-growing and low-grade cancer type, although some types of PCa can become aggressive and turn to metastatic castration-

 doi:10.20944/preprints202603.2479.v1

resistant prostate cancer (mCRPC) [1]. The slow-growing nature of PCa also renders a problem in establishing prostate cancer animal models, especially subcutaneous xenografts that can take more than 2 months (volume doubling time is 86 hours) to form the tumors [2]. In many cases, no measurable tumor formation occurs even after a prolonged period. Such slow kinetics and ambiguous outcomes limit throughput for preclinical screening, delay longitudinal imaging studies, and increase animal housing and maintenance costs. Therefore, a real-time, non-invasive approach would be valuable for tracking the growing potential of human PCa cells in xenograft model, and is essential for accurately assessing the efficacy of novel therapeutic strategies.

Recent advances in molecular imaging and targeted radionuclide therapy have revolutionized prostate cancer management. Reporter gene imaging (RGI) is defined as delivery of one or multiple functional genes expressing fluorescent proteins, bioluminescent enzymes or functional proteins into cells of interests to be detected by optical imaging or radionuclide-based imaging such as PET/SPECT [3]. Although retroviral mediated transduction can better stabilize reporter genes in cells via chromosomal integration, it is challenged by eliciting both intended and unintended immune responses [4,5]. In addition, viral gene delivery requires the presence of polybrene, which may cause cytotoxicity with lentiviral transduction [6,7]. On the other hand, non-viral delivery of reporter genes via electroporation, liposomes, and cationic polymers is relatively safe and less possible to induce severe immune response, while the gene delivery is temporary and low stability [4,5,8,9]. The advantage and disadvantage of viral and non-viral systems has been reported to be compromised using DNA transposon gene delivery by non-viral transduction of a dual plasmid system, including a transposase vector and a gene of interest flanked by inverted terminal repeats (ITR) [10,11]. *PiggyBac* transposon system has been reported to exhibit highest transposition activity and low overproduction inhibition compared to other transposon system in mammalian cells [12,13]. This system has been reported to establish stable cell lines with multiple reporter genes in murine breast cancer cells and human hypopharyngeal cancer cells. Despite the transfection efficiencies of both cell types are low, the transfected cells can be enriched by the flow cytometry and express long-term reporter gene activity [14,15]. For monitoring the progression and therapeutic responses of slow growth kinetics cancer such as PCa, RGI should be convenient and cost-effective for long-term and repeatedly tracking the tumor growth in vivo, especially the orthotopic tumor model. It is speculated that *PiggyBac* transposon system is appropriate for establishing stable PCa cells for long-term preclinical investigation because of low immunogenicity and high stability of reporter gene activity.

Prostate-specific membrane antigen (PSMA) has emerged as a robust molecular target for both diagnosis and therapy. ^{68}Ga-PSMA PET/CT enables sensitive detection of recurrent and metastatic lesions, while ^{177}Lu-PSMA-617 has demonstrated significant improvements in overall survival in patients with mCRPC, and it has been approved by the USA Food and Drug Administration (FDA) and European Medicines Agency [16,17]. Despite these advances, the translation of novel theranostic strategies remains limited by deficiency of ideal preclinical models. Particularly, combination of external beam radiotherapy (EBRT) or immunotherapy with ^{177}Lu-PSMA-617 has been considered promising for PCa treatment, while a robust and reliable small-animal validation remains essential for preclinical and translational investigation [18-20]. Most murine tumor models used for assessing the efficacy of ^{177}Lu-PSMA-617 monotherapy or combination therapy are subcutaneous xenograft inoculation using PSMA positive LNCaP cells or PSMA transduced PC3 cells (PC3-PIP) with slow growth kinetics [19,21-23]. the Surprisingly, prostate directed orthotopic tumor model is rarely reported in related studies, although it is believed that the microenvironment and tumor stromal interaction should better mimic the development of PCa cells [23]. However, the technical difficulty in anatomic engrafting and real-time monitoring of tumor progression remains a challenge for using this important preclinical model.

In this study, we have transduced a *PiggyBac* transposon system carrying triple reporter genes, including an improved luciferase gene (*luc2*), a red fluorescence protein gene (*RFP*), and a herpes simplex virus type I thymidine kinase gene (*HSV1-tk*) into human C4-2 PCa cells, which are isolated from a subcutaneous LNCaP formed xenograft tumor. The established C4-2 3R cells were compared

 doi:10.20944/preprints202603.2479.v1

for their tumor formation capacity in subcutaneous xenograft model and prostate orthotopic model using the bioluminescence imaging. Moreover, the orthotopic tumor model with C4-2 3R cells was applied to assess the tumor responses after a single treatment of ^{177}Lu-PSMA-617, X-rays irradiation, and a combination of both regimens. Current data proved that C4-2 3R cells exhibited robust growth kinetics in the orthotopic model, and was easy to be tracked for the tumor responses in vivo after versatile therapeutic approaches.

Materials and Methods

Cell Culture

Human prostate cancer C4-2 cells were purchased from American Type Culture Collection (Cat# CRL-3314, ATCC, Manassas, VA, USA). Cells were cultured in Roswell Park Memorial Institute (RPMI) 1640 medium (Gibco® ThermoFisher Scientific, Waltham, MA, USA) supplemented with 10% fetal bovine serum (FBS, HyClone® ThermoFisher Scientific, Waltham, MA, USA), 1% penicillin-streptomycin solution (100X) (Gibco® ThermoFisher Scientific, Waltham, MA, USA) and 1% L-glutamine (200mM) (Sigma-Aldrich Co., St. Louis, MO, USA). Cells were maintained in 37℃ incubator filled with 5% CO2 in air and were passaged every two days. C4-2 3R cells were cultured with identical condition after they were established.

Preparation of Radiopharmaceuticals

PSMA-617 was obtained from MedChemExpress (MCE, Cat#HY-117410, NJ, USA). PSMA-617 (10 mM in DMSO), sodium acetate (0.4M, pH 5.5), 20% ascorbic acid solution, and ^{177}Lu-LuCl3 (Isotopia, Israel) were added to a reaction vial. The reaction mixture was allowed to react at 95°C for 60 min. After the reaction, the crude product was loaded onto a C18 Sep-Pak cartridge, which was preconditioned with 10 mL of ethanol, followed by 10 mL of ddH2O. The desired compound was eluted using an ACN/H2O solution (1:1, vol/vol). Labeling efficiency was assessed by radio-thin layer chromatography (radio-TLC, AR2000, Bioscan) system using instant thin layer chromatography (ITLC) plates (Merck, Darmstadt, Germany) as the stationary phase and using 0.5 M sodium citrate buffer (pH = 5.0) as the mobile phase. The radiochemical purity of ^{177}Lu-PSMA-617 was required to exceed 90% for use in subsequent experiments. ^{18}F-PSMA-1007 was purchased from Department of Nuclear Medicine, Taipei Veteran General Hospital.

Transfection of PiggyBac Transposon Constructs and Cell Sorting

The *PiggyBac* transposon plasmid named PB-3R-puro has been constructed as reported before [24]. This plasmid was co-transfected with Act-PBase plasmid [25] into C4-2 cells using PolyJet™ reagent (SignaGen, Frederick, MD, USA) by following the manufacturer's protocol. The ratio of PB-3R-puro and Act-PBase was 4:1 mixed in 5 g total plasmids for transfection. After transfection for 48 hours, mRFP expressing cells were visualized under the fluorescent microscope (CKX53, Olympus, Hachioji, Japan). Subsequently, transfected C4-2 cells were sorted using the flow cytometry (CytoFLEX SRT, Beckman Coulter, Brea, CA, USA). In brief, 1×10^7 cells were resuspended in the fluorescence activated cell sorting (FACS) buffer (1% FBS in phosphate buffered solution buffer) and injected into the flow cytometer to sort out the red fluorescent cells for enrichment. Sorted cells were routinely passaged and visualized using the fluorescent microscope to confirm the expression of mRFP reporter protein.

Luciferase Reporter Gene Assay

Cells (1×10^5) were mixed with 100 µL RPMI 1640 with 5 repeats in wells of a 96-well plate (Cat# 655083, CELLSTAR®, Greiner Bio-One, Kremsmünster, Austria). Each well was then mixed with 100 µL of 15 mg/mL D-luciferin (Cat# LUCK-1G, GOLDBIO, MO, USA) and subjected to the ELISA reader (Infinite® 200 PRO, TECAN, Seestrasse, Männedorf Switzerland).

 doi:10.20944/preprints202603.2479.v1

Cell Viability Assay

Cells ($1x10^4$) were seeded in a 96-well plate, and then treated with escalating concentrations (0-40 M) of ganciclovir (GCV, Sigma-Aldrich Co., St. Louis, MO, USA) for 4 days. Subsequently, 1mg/ml MTT solution (3-[4,5-dimethylthiazol-2-yl]-2,5-diphenylterazoliumbromide, Sigma-Aldrich Co., St. Louis, MO, USA) was added in medium without FBS for 3 hours. Cells were added with 100 μL of dimethyl sulfoxide (DMSO) to dissolve crystals after removal of MTT solution. The plate was placed in an ELISA reader (Sunrise, TECAN Group Ltd., Männedorf, Switzerland) and scanned by 570 nm of absorbed wavelength.

X-Rays Source

Radiation exposure was performed using a cabinet X-rays irradiator (X-Rad 225XL, Precision, Madison, CT, USA). The dose rate is 134.3cGy/min.

Establishment of Tumor Models in Small Animals

Five-week old Balb/C nu/nu male mice (BALB/cAnN.Cg-Foxn1^{nu}/CrlNarl) were purchased from (National Laboratory Animal Center, NLAC, Nankang, Taiwan). Mice were hospitalized for one week before tumor inoculation. For orthotopic tumor model, C4-2 3R cells ($2x10^5$) were resuspended in 20 L of Matrigel® (Cat # 354248, Corning, Glendale, AZ, USA) and OPTI-MEM (Gibco® ThermoFisher Scientific, Waltham, MA, USA) solution in 1:1 ratio, and gently injected into the surgical exposed prostate as reported previously [26]. In brief, mice were anesthetized using 3% isoflurane. Sterilized surgical instruments was used in whole process. The lower abdomen was disinfected with 70% ethanol followed by povidone–iodine. Approximately 1 cm midline incision was made in the lower abdomen. The seminal vesicles and bladder were gently exteriorized using a sterile cotton swab to locate the prostate. After injection, the muscle layer was closed using sterile absorbable 6-0 chromic gut sutures (Cat# CC126, UNIK, New Taipei, Taiwan), and the skin was closed with sterile non-absorbable 4-0 nylon sutures (Cat# NC124, UNIK). The incision site was disinfected with povidone–iodine, and mice were monitored daily for one week to assess wound healing. For subcutaneous xenograft tumor model, $1×10^7$ cells were resuspended in 100 L Matrigel® and OPTI-MEM mixture, and subcutaneously injected into right thigh of each mouse with anesthesia. The animal cares and experiments have been approved by Institutional Animal Care and Use Committee of National Yang Ming Chiao Tung University (Approval IACUC number: 1121202).

Bioluminescence Imaging

Tumor-bearing mice (N=8 for tumor growth tracking, N=12 for therapeutic evaluation) were intraperitoneal injected with 150 mg/kg D-luciferin (Caliper Co., Hopkinton, MA, USA) and were anesthetized using 2 % isoflurane during image acquisition. The mice were then placed in the IVIS Lumina X5 (PerkinElmer, Life and Analytical Sciences Inc., Waltham, MA, USA) for acquiring luminescent signals at the region of interests (ROIs). The photon fluxes were semi-quantified as photons/sec using the bundled Living Imaging® software (ver. 4.7.4, Revvity, Waltham, MA, USA).

Micro-Magnetic Resonance Imaging (MRI) for Small Animals

MRI was performed using a 7T PET/MR Inline (Bruker, Rheinstetten, Germany). A T2-weighted TurboRARE sequence was used to monitor the position of prostate tumor five weeks after tumor implantation. Tumor-bearing mice were anesthetized with 3 % isoflurane. The depth of anesthesia, pulse and respiration were continuously monitored throughout the imaging procedure. The sequence parameters included: echo time (TE) = 27.82 ms, repetition time (TR) = 2177 ms, echo train length (ETL) = 8, average = 8, slice thickness = 1 mm, field of view 35 × 35 mm, matrix size 192 × 192, in-plane resolution 156 × 156 μm, 30 slices, and 7 minutes of acquisition time.

 doi:10.20944/preprints202603.2479.v1

Preparation of Membrane Proteins

The subcellular protein fractionation kit for cultured cells (ThermoFisher Scientific, Waltham, MA, USA) was used to separate membrane proteins and cytoplasmic proteins according to the manufacturer's instruction.

Western Blot Analysis

Cell lysates were extracted using protein lysis buffer (50 mM Tris-HCl, 120 mM NaCl, 0.5% NP-40) supplemented with 2% proteinase inhibitor (Sigma-Aldrich Co., St. Louis, MO, USA), and mixed at 4 ˚C for 15 minutes followed by centrifugation for another 15 minutes. Proteins were quantified using the Bio-Rad Protein Assay reagent (Bio-Rad, Bio-Rad Laboratories Inc., Hercules, CA, USA). To separate proteins, samples were boiled in the sampling buffer [250 mM Tris-HCl pH6.8, 10% sodium ddecyl sulfate (SDS), 30% glycerol, 5% β- mercaptoethanol, and 0.02% bromophenol blue], and run on a 10% SDS-polyacrylamide gel electrophoresis gel (SDS-PAGE) at 90 volt for 100-120 minutes. The gel was then electro-transferred to a nitrocellulous membrane (BioTrace™NT, Pall, Port Washington, NY, USA), which was blocked in TBST buffer (150 mM NaCl、10 mM Tris-HCl、0.1% Tween 20，pH 8.0) containing 4% skim milk. The membrane was detected using different primary antibodies, including anti-PSMA (Cat# 12072, Cell Signaling Technology Inc., Beverly, MA, USA), anti-Na^+/K^+ ATPase (Cat# ab76020, Abcam, Cambridge, MA, USA), anti- -tubulin (Cat# GTX112141, GeneTex Inc., Alton Pkwy Irvine, CA, USA), and anti-glyceraldehyde 3-phosphate dehydrogenase (GAPDH, Cat# MA5-15738, Invitrogen Inc. Carlsbad, CA, USA). The secondary antibody is horseradish peroxidase (HRP)-conjugated anti-rabbit or anti-mouse IgG (Millipore Co., Billerica, MA, USA). The membrane was rinsed with Trident femto Western HRP substrate (Genetex Inc., Irvine, CA, USA) and detected for the chemoluminescent signals using the ImageQuant™ LAS-4000 (GE Healthcare Bio-Science AB, Uppsala, Sweden). The intensity of protein bands was quantified by densitometric function of ImageJ software (Version 1.47).

Flow Cytometric Analysis of PSMA

Cells ($1.2x10^6$) were cultured for 24 hours, and then exposed to different doses of X-rays. Cells were re-incubated for 4 hours, and then collected in FACS buffer. After centrifugation, pellets were mixed with Alexa Fluor® 488 anti-human PSMA antibody (IgG isotype, Cat# 342506, Biolegend, San Diego, CA, USA) diluted in FACS buffer (1:100) on ice for 1hour. Cells were spun and resuspended in 500 L FACS buffer and sieved through a 37 m mesh. The samples were subjected to the flow cytometer (CytoFlex, Beckman Coulter, Brea, CA, USA) to detect the fluorescent signals, and the results were normalized to 0 Gy.

Immunofluorescence Microscopy

Cells seeded on coverslips were incubated with PBS diluted Lipophilic Tracers-DiI (Cat # D282, Thermo Fisher Scientific, Waltham, MA, USA) for staining of cell membrane. Subsequently, stained cells were fixed with 4% paraformaldehyde for 10 minutes, and then blocked in 5% bovine serum albumin (BSA) for 1 hour. The Alexa Fluor® 488 anti-human PSMA antibody (IgG isotype, Cat# 342506, Biolegend) was diluted in 5% BSA (1:100) and reacted with cells on the coverslips for 12 hours. Cell nuclei were stained with 2 μg/mL 4',6-diamidino-2-phenylindole (DAPI), mounted and sealed on the slide for imaging acquisition using the confocal microscope and analyzed by bundled ZEN3.1 software (ZEISS LSM 880, Oberkochen, Germany).

Radiation Exposure and Radioligand Therapy on Orthotopic Tumors

For X-rays irradiation, tumor-bearing mice (N=3 for untreated control and each experimental group) were anesthetized with 2% isoflurane and positioned supine on the platform for receiving a 2 Gy dose using a cabinet X-ray irradiator. The lower abdomen was centered within the irradiation field, while the remaining body regions were shielded with lead blocks to protect normal organs. For

 doi:10.20944/preprints202603.2479.v1

PSMA-targeted radioligand therapy, mice were administered a single dose of 14.8 MBq of ^{177}Lu-PSMA-617 via tail-vein injection. For combined treatments, mice received the same dose of ^{177}Lu-PSMA-617 4 hours after 2Gy X-ray irradiation to evaluate the impact of radiation pre-treatment on therapeutic efficacy. Body weight was measured every two days to assess treatment-related toxicity and overall health status.

Positron Emission Tomography/Computed Tomography (PET/CT) for Small Animals

Expression of PSMA in tumor-bearing mice with different treatments was detected using animal PET/CT (Mediso nanoScan® PET/CT, Budapest, Hungary) serviced by Molecular Translational Imaging Center in Chang-Gung Memorial Hospital, Linkou, Taiwan. Mice were administered a single dose of 11.1 MBq of ^{18}F-PSMA-1007 via tail-vein injection. After one hour, the mice were imaged by animal PET/CT for 15 minutes with 2% isoflurane anesthesia. The scanned images were analyzed using Pmod software (Pmod Version 4.4, Bruker, Billerica, MA, USA).

Hematoxylin and Eosin (H&E) Staining

Tumor tissues were harvested, rinsed briefly in PBS, and fixed in 10% neutral-buffered formalin for 24 hours at room temperature. After fixation, samples were dehydrated through a graded ethanol series, cleared in xylene, and embedded in paraffin. Paraffin blocks were sectioned at a thickness of 3 μm using a rotary microtome and mounted onto glass slides. For staining, sections were deparaffinized in xylene and rehydrated through graded ethanol (100%, 95%, 75% for 3 minute each) to distilled water. Slides were incubated in hematoxylin for nuclear staining, rinsed in running tap water, and differentiated in acid alcohol if necessary. After bluing in alkaline solution, sections were counterstained with eosin. Slides were then dehydrated through ascending ethanol concentrations, cleared in xylene, and coverslipped using a synthetic resin mounting medium. Stained sections were examined and imaged using a bright-field microscope equipped with a digital camera.

Statistical Analysis

The statistical analysis was assessed by Student's t-test, and $p<0.05$ was regarded statistically significant. Prism v10.1 (GraphPad Software DBA Statistical Solutions, Franklin St FL Boston, MA, United States) was used to plot the data.

Results

Establishment and Validation of PiggyBac Transposon System Mediated Delivery of Triple Reporter Genes into C4-2 Cells

The arrangement of triple reporter genes with a puromycine resistant cassette flanked by 5′ and 3′ internal terminal repeat (ITR) in *PiggyBac* construct was diagramed (Figure 1A). C4-2 cells were transfected with the *PiggyBac* construct as described in materials and methods. The transfection efficiency of C4-2 cells was approximately 7% as visualized by fluorescent microscopy and counted by flow cytometry, and mRFP expressing cells were then sorted by FACS and enriched after sub-culture (Supplementary Figure 1A-D). Although C4-2 3R cells were not selected by puromycine, they could still stably express mRFP after routine passage compared to parental C4-2 cells (Figure 1B). The expressions of *luc2* and *HSV1-tk* reporter genes in C4-2 3R cells were further demonstrated by luciferase assay and MTT assay, respectively. The results demonstrated that C4-2 3R cells expressed robust luciferase activity (Figure 1C). These cells also exhibited significant cytotoxicity after treated with 5-20 M GCV, a nucleotide analog that can be phosphorylated by HSV1-tk and interfere DNA synthesis (Figure 1D). Despite the proliferative rate of C4-2 3R cells was slower than parental C4-2 cells, the doubling time still reached 21 hours (Supplementary Figure 1E).

 doi:10.20944/preprints202603.2479.v1

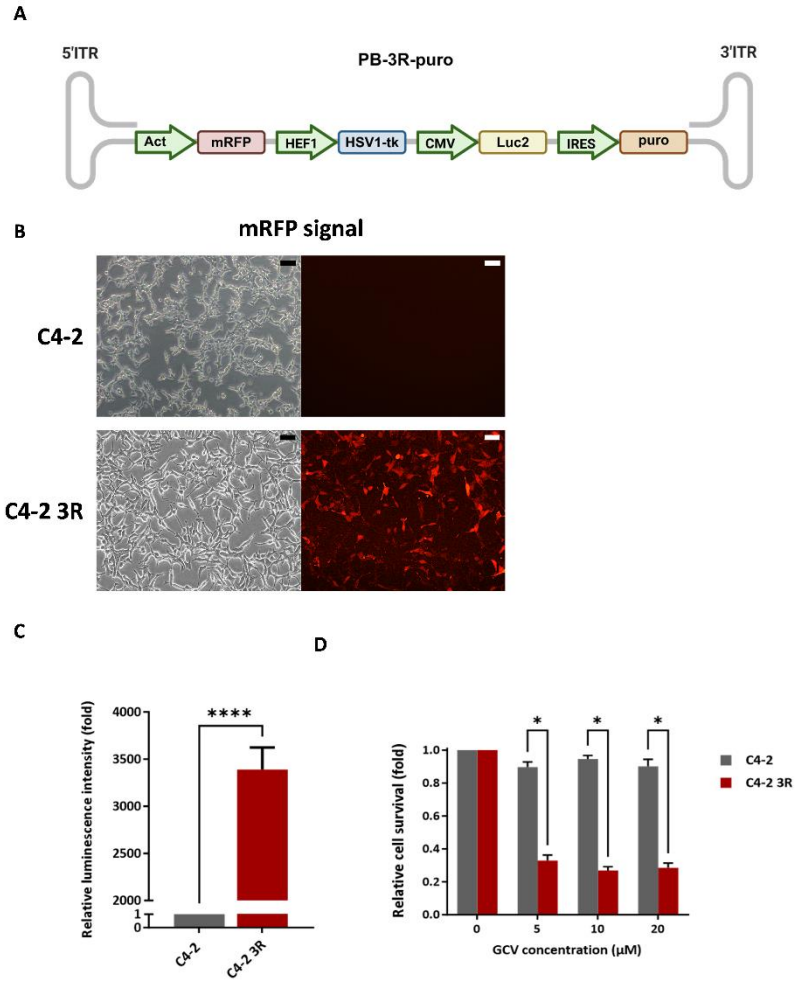

Figure 1. Establishment of C4-2 3R cells. (A) An illustration of triple reporter genes cassette arranged in the PB-3R-puro construct; (B) visualization of C4-2 cells and C4-2 3R cells using the fluorescence microscope; (C) detection luciferase activity using the luciferase assay; (D) assessment of GCV toxicity in HSV1-tk reporter gene expressing Cells using the MTT assay. *: $p<0.05$; ****: $p<0.0001$.

RGI of Tumor Formation in Orthotopic Model and Subcutaneous Xenograft Model Using C4-2 3R Cells

C4-2 cells are tumorigenic in immune deficient male nude mice as reported by ATCC (https://www.atcc.org/products/crl-3314#detailed-product-information). To better understand the tumor formation capacity of C4-2 3R cells in vivo, we performed an orthotopic inoculation of C4-2 3R cells as diagramed (Figure 2A). The surgical procedure of intraprostatic injection of C4-2 3R cells were recorded by photos (Supplementary Figure 2). Photo imaging was taken to demonstrate the placement of the tumor injection within the prostate. (Figure 2B). To track the tumor growth kinetics, we performed the bioluminescence imaging to monitor the change of photon flux of C4-2 3R cells in orthotopic tumor weekly. It showed that the bioluminescent signals of tumor-bearing mice gradually increased up to 5 weeks, even though the signal intensity varied in each mouse (Figure 2C). The photon fluxes of orthotopic tumors were semi-quantified to verify the trend of tumor growth (Figure 2D). Additionally, 7T MRI with T2 weighted sequence was used to validate the bioluminescent signal at one of the fifth-week tumors (Figure 2E). We also performed the subcutaneous xenograft model using C4-2 3R cells. Although we could detect the bioluminescent signals in mice after inoculation for one week, they were not sustained or propagated after 5 weeks of tracking (Figure 2F and 2G). The subcutaneous xenograft tumors eventually never formed up to 8 weeks of examination (data not shown).

 doi:10.20944/preprints202603.2479.v1

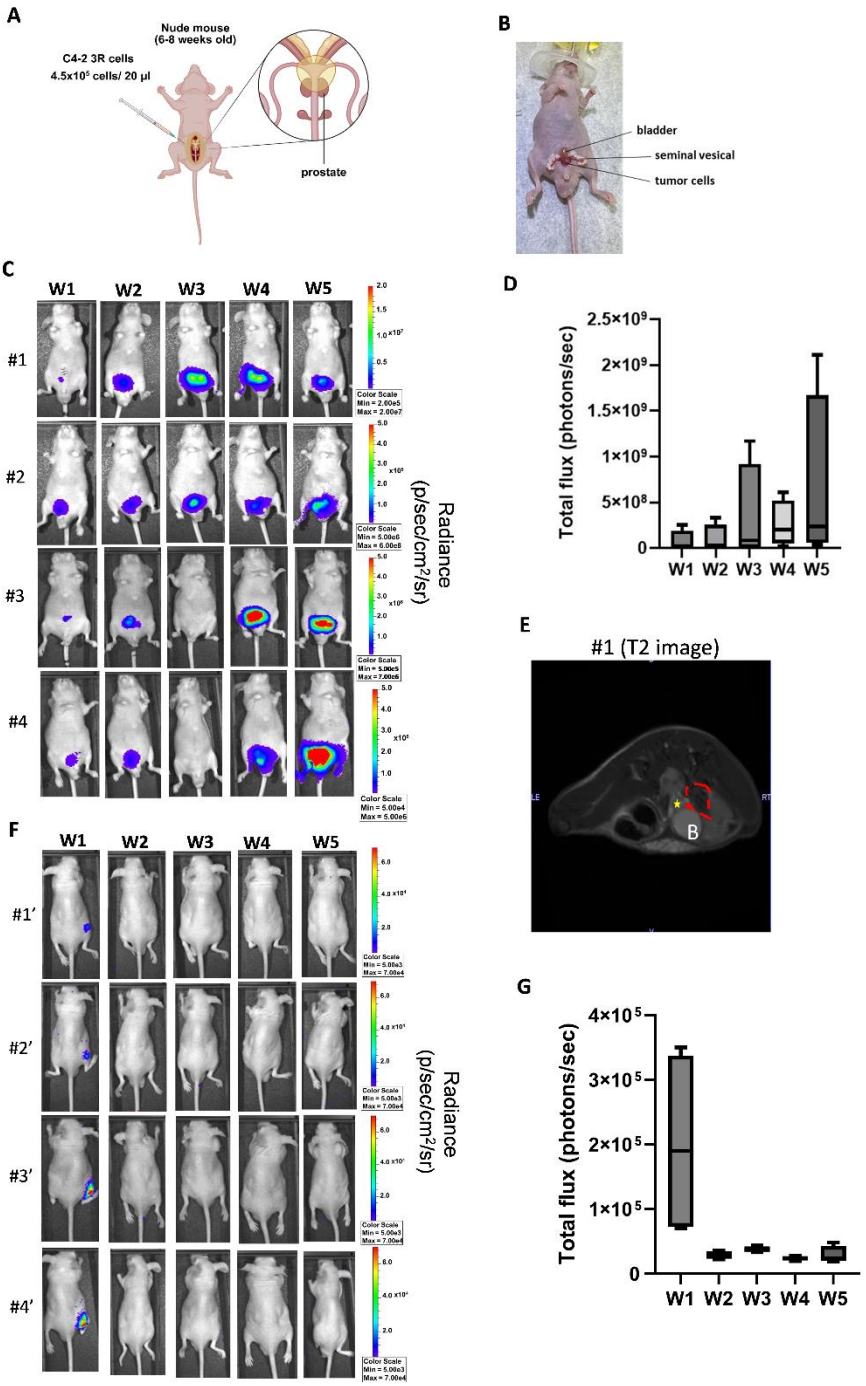

Figure 2. Establishment of PCa tumor models for monitoring of tumor progression by bioluminescent imaging. (A) A representative diagram of C4-2 3R cells inoculation into prostate; (B) a photo demonstration after cells were inoculated in prostate; (C) bioluminescence imaging of C4-2 3R orthotopic tumors weekly; (D) semi-quantification of total photon flux of bioluminescence imaging in the orthotopic tumor model; (E) T2-weighted image for the tumor-bearing mouse (#1) at fifth week. The tumor position was indicated by the dotted circle. B: bladder; asterisk: prostate; (F) bioluminescence imaging of C4-2 3R subcutaneous xenograft tumors weekly; (G) semi-quantification of total photon flux of bioluminescence imaging in the subcutaneous xenograft tumor model.

Assessment of PSMA Expression After X-Rays Irradiation in C4-2 Cells

It has been reported that X-ray EBRT can temporarily up-regulate the expression of PSMA gene in LNCaP cells [19]. Although C4-2 cells are derived from LNCaP cells formed subcutaneous xenograft tumor, it has been reported that they exhibit enhanced radioresistant property by increasing cell cycle arrest and DNA repair relevant genes [27]. Therefore, it is still essential to confirm

 doi:10.20944/preprints202603.2479.v1

the radiation response of PSMA in C4-2 cells that would influence the application of C4-2 3R cells on PSMA-targeting radioligand therapy (TRT) and combined treatment in orthotopic tumor model. We first irradiated C4-2 cells with 2 to 8 Gy X-rays to examine the expression of total PSMA protein. Surprisingly, no PSMA level change was found in this dose range after 4 hours of exposure (Figure 3A). As PSMA is a membrane protein, we isolated cell membrane to examine the change of PSMA after 4 hours of irradiation. The results showed that membrane PSMA was equivalently increased after 2 to 8 Gy exposure accompanied by decrease of cytoplasmic PSMA compared to un-irradiated cells, except 4 and 8 Gy that showed little change in cytoplasmic PSMA (Figure 3B). The expression of membrane PSMA was also validated using flow cytometric analysis, and it showed that radiation tended to increase the level of membrane PSMA in C4-2 cells (Figure 3C). Quantification of flow cytometric data revealed that 2 and 6 Gy X-rays irradiation induced more significant increase of membrane PSMA positive cells compared to un-irradiated cells (Figure 3D). Moreover, the fluorescent microscopy was used to visualize the membrane PSMA, which could be detected in cells exposed to X-rays, especially 2 to 6 Gy but was less visualized in un-irradiated cells (Figure 3E). Taken together, ionizing radiation tends to promote the relocation of PSMA to cell membrane rather than increase of total PSMA in C4-2 cells.

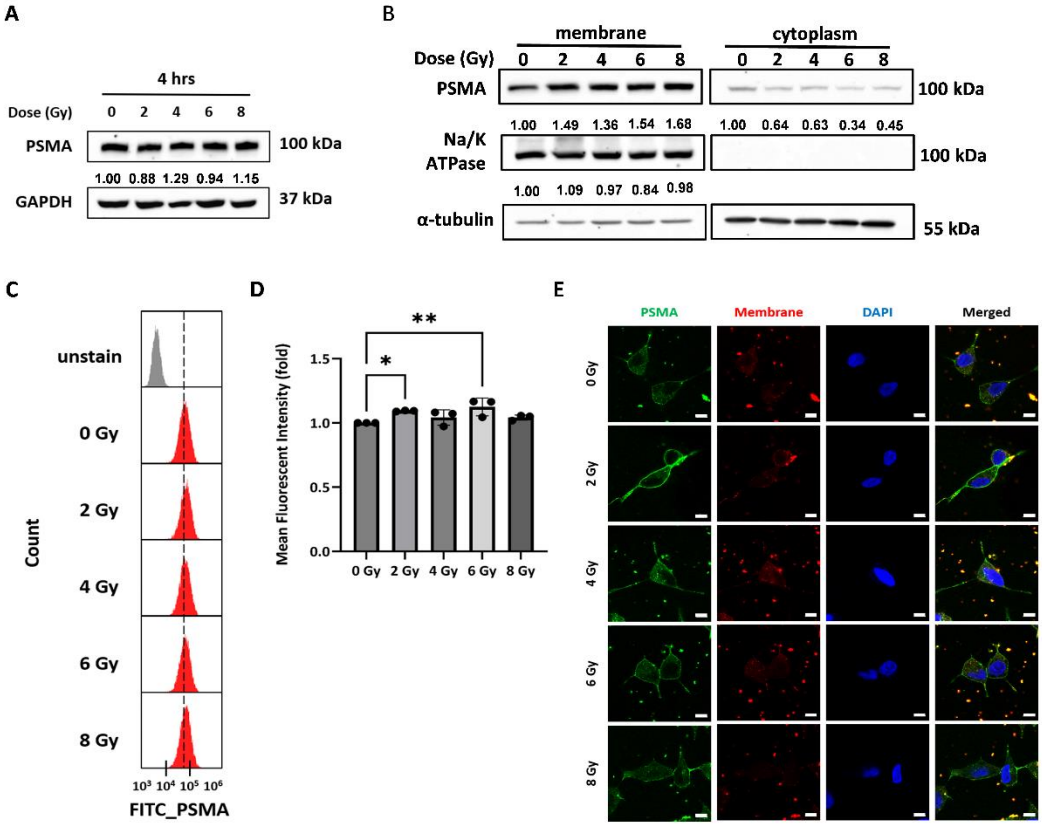

Figure 3. X-rays irradiation induced membrane PSMA in C4-2 cells. (A) Western blot analysis of total PSMA in C4-2 cells exposed to different doses or X-rays; (B) analysis of PSMA expression in cell membrane and cytoplasm; (C) flow cytometric analysis of PSMA on cell surface; (D) quantification of PSMA signals from the flow cytometry; (E) immunofluorescence imaging of PSMA expression 4 hours after C4-2 cells exposed to different doses of X-rays. Scale bar: 10 m. *: p<0.05; **: p<0.01.

 doi:10.20944/preprints202603.2479.v1

Potential of C4-2 3R Cells on Evaluation of Combined X-Ray EBRT and ^{177}Lu-PSMA-617 Radioligand Therapy In Vivo

The C4-2 3R cells established orthotopic prostate tumor model for therapeutic assessment of EBRT and ^{177}Lu-PSMA-617 was schemed (Figure 4A). After tumors were formed for 5 weeks, monotherapy and combination of 2 Gy X-rays and ^{177}Lu-PSMA-617 were separately applied in tumor-bearing mice, and PET/CT using ^{18}F-PSMA-1007 was firstly used to evaluate the expression of PSMA in orthotopic tumors after one week of treatments (Figure 4B). The PET/CT images were quantified and showed that average SUV of combined treatment was significantly higher than that in the untreated control and ^{177}Lu-PSMA-617 monotherapeutic group (Figure 4C). The responses of tumors to various treatments were measured by bioluminescence imaging for two weeks, and the results showed that photon signals in orthotopic tumors were significantly reduced in combined X-rays and ^{177}Lu-PSMA-617 compared to either monotherapy (Figure 4D). Photon flux was semi-quantified for each treatment group between weeks 5 and 7 (Day 0 and 14 of treatments, respectively), and the combination therapy resulted in a significantly greater reduction in bioluminescent signal compared with ^{177}Lu-PSMA-617 alone (Figure 4E). Therefore, C4-2 3R cells have displayed capacity for establishment of trackable orthoptic prostate tumor model that can be used for investigating preclinical efficacy of novel therapeutic strategies.

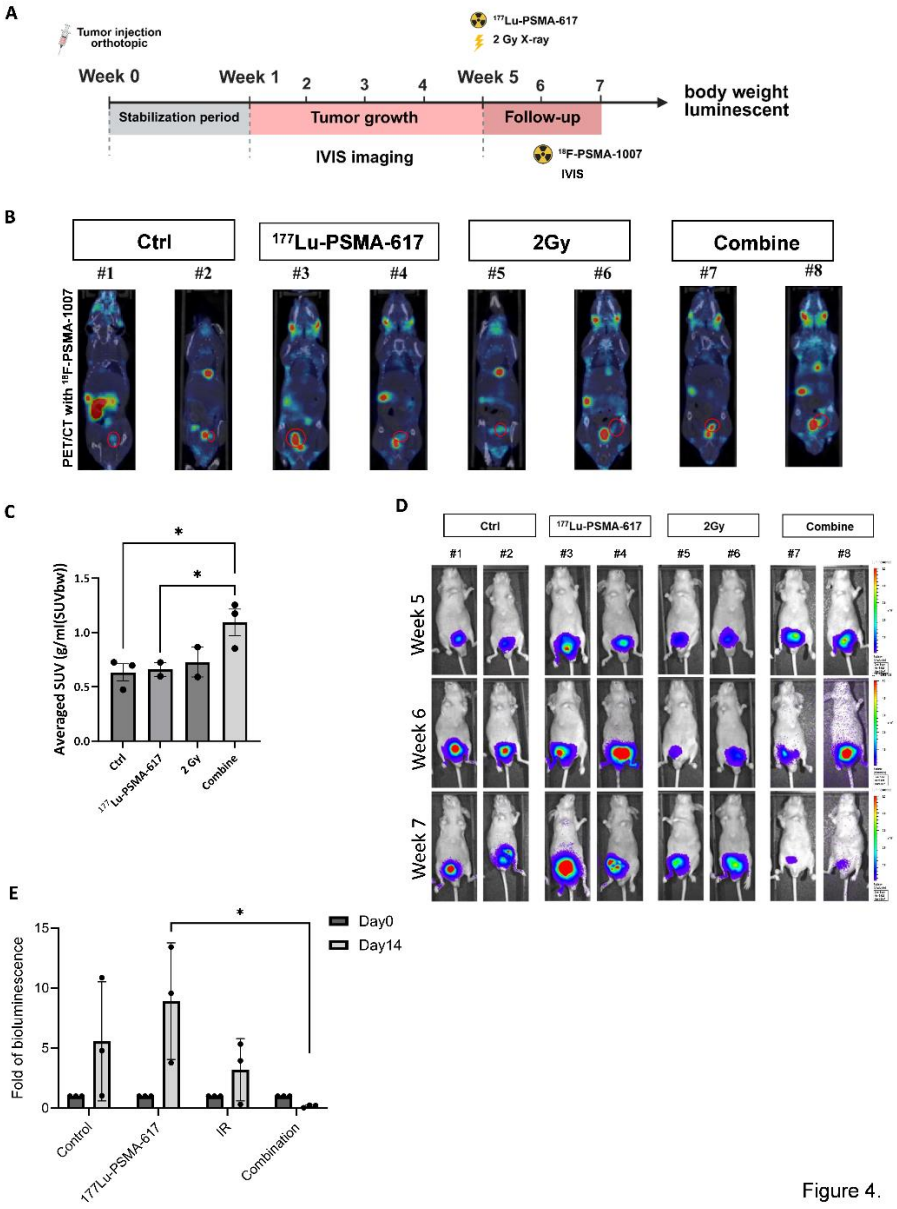

Figure 4.

 doi:10.20944/preprints202603.2479.v1

Figure 4. C4-2 3R orthotopic tumor model for monitoring the tumor responses to X-rays and ^{177}Lu-PSMA-617 treatments. (A) A scheme of orthotopic tumor model for examination of tumor responses to different treatments using molecular imaging; (B) PET/CT imaging of tumor uptake for ^{18}F-PSMA-1007 tracer after different treatments; (C) quantification of average SUV in PET/CT imaging; (D) bioluminescence imaging of tumor responses to different treatments; (E) semi-quantification of photon signals in bioluminescence imaging. Ctrl: untreated control. *: $p<0.05$.

Dissection of C4-2 3R Cells Formed Orthotopic Tumor Tissue with Different Treatments

After the final imaging acquisition, tumors grew in prostate with different treatments were dissected from tumor-bearing mice for comparison. C4-2 3R cells formed tumors in the combined treatment group appeared substantially smaller than those in the monotherapy or control groups (Figure 5A). The dissected tissues were also subjected to preparation of tissue sections and histological examination. It showed that heavy staining of tumor tissues was mainly detected in untreated control, while different types of treatments could lead to reduced tumor staining to different levels (Figure 5B).

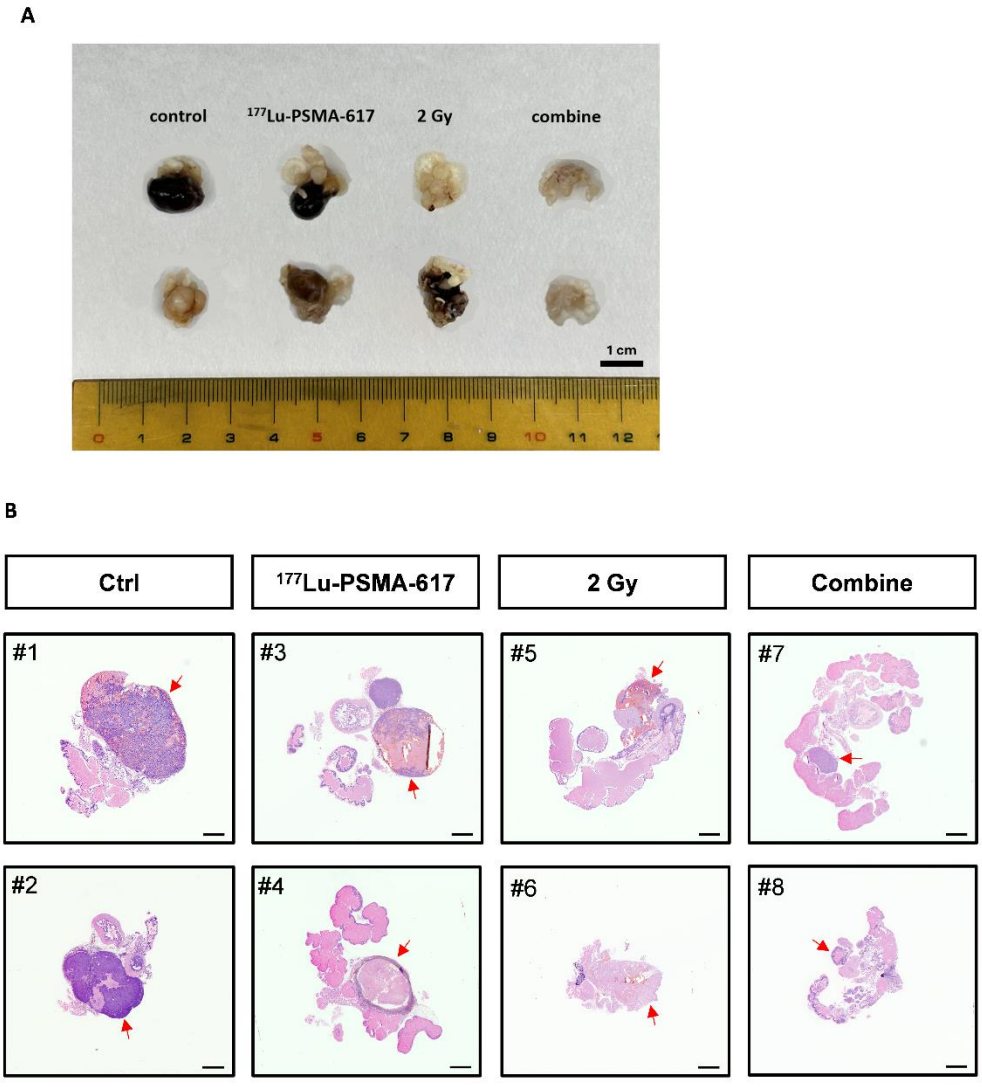

Figure 5. Dissection of C4-2 3R cells formed tumors from orthotopic prostate tumor model. (A) Orthotopic tumors excised from tumor-bearing mice after different treatments for 5 weeks. The numbers represent the mice indicated in Figure 4. Scale bar: 1cm; (B) H & E staining of tumor sections from different treatments. The tumor positions were indicated by arrows. Ctrl: untreated control. Scale bar: 2000 m.

 doi:10.20944/preprints202603.2479.v1

Discussion

The slow growth nature of prostate cancer translates into correspondingly slow tumor development in xenograft models. LNCaP cells are commonly used for establishment of subcutaneous xenograft tumor model, while it usually requires 2 to 3 months to form palpable tumors, and tumor growth may remain modest or regress without continuous androgen supplementation [2,28]. On the other hand, the orthotopic prostate cancer model is believed to provide a better organ associated microenvironment for tumor development, while the technical demanding is a limitation to establish this tumor model [29,30]. It has been reported that using microscope-guided orthotopic injection of LNCaP cells will generate a more promising result, but it also requires advanced anatomic knowledge on mouse prostate and proper technique as well as instruments [31]. Additionally, the orthotopic tumor growth can only be tracked by ultrasound (US) or MRI, which depends on the well-trained and experienced radiographers and operators to interpret data. Importantly, the unpredictability of slow-growing prostate cancer models reflects clinical diagnostic uncertainty, where limited biopsy sampling may underestimate tumor grade and result in postoperative upgrading. Extended-core biopsy has demonstrated to improve detection accuracy and reduce upgrading risk [32], highlighting the impact of sampling strategy on risk stratification.

In this study, we introduced RGI to provide a simple and user-friendly approach for monitoring the growth kinetics as well as the therapeutic evaluation. C4-2 PCa cells are derived from LNCaP cells, but they have not been reported to be used for orthotopic tumor model, except C4-2B cells derived from C4-2 with greater propensity for androgen-independent growth and bone metastasis [33]. C4-2 3R cells established tumor model could be started to monitor as early as one week after tumor inoculation. Especially, bioluminescence imaging is a functional imaging that the photon signals represent viable tumors compared to anatomic imaging like US and MRI. Thus, it would be easy to determine if the implanted tumors have eventually grow for further study, or another round of animal study should be schemed earlier to avoid time wasting. Although *luc2* expressed in C4-2 3R cells was primarily used to demonstrate the capacity of bioluminescence imaging in orthotopic PCa tumor model, this cell type also harboring *mRFP* and *HSV1-tk* that would be used for in vivo fluorescent imaging and radionuclide imaging, respectively [34]. The multimodality molecular imaging potent of C4-2 3R cells may contribute to establish non-invasive and real-time trackable orthotopic PCa model that can be used for time-saving and reliable preclinical model for theranostic assessments.

Before use of *PiggyBac* transposon system, we have referred to a previously established C4-2-luc cells using viral transduction for triple reporter genes [35]. However, C4-2 cells could not survive after transduction, which might be caused by high polybrene sensitivity [36]. Indeed, the *PiggyBac* transposon system possesses several advantages compared to viral transduction, including larger cargo, less time-consuming and laborious, and reliable genomic integration even cells with low transfection efficiency [14,15,24,37]. To the best of our knowledge, this is the first demonstration that *PiggyBac* transposon system can successfully deliver reporter genes to C4-2 cells that fail to accept viral transduction.

PSMA is an important target for theranostic treatment of PCa. However, PSMA expression has been reported to be low or deficient in about 30% of mCRPC [38]. Therefore, induction of PSMA expression would be interesting and important for clinical application. EBRT is a common clinical therapy used for PCa treatment, and a recent report has demonstrated that EBRT can increase the expression of PSMA gene and enhance the uptake of ^{177}Lu-PSMA-617 using LNCaP subcutaneous xenograft tumor model, while the data show high variability [19]. Moreover, radiation induced PSMA expression is associated with double-strand DNA damage as topoisomerase-2 inhibitors also exhibit similar effect in LNCaP cells [39]. While subcutaneous xenograft tumor model was used for these studies, we further used C4-2 3R cells established orthotopic tumor model to validate the increased PSMA levels by PET/CT imaging. Mechanically, we found that C4-2 cells did not increase the expression of PSMA after X-rays irradiation, but promote the membrane relocation of PSMA. Radiation exposure is well known to activate DNA damage response (DDR) signaling pathways,

 doi:10.20944/preprints202603.2479.v1

including ATM/ATR kinase activation and γH2AX formation [40,41]. It is therefore possible that the observed PSMA membrane relocalization represents a broader radiation-induced cellular stress adaptation rather than direct transcriptional upregulation. Previous studies have also suggested that radiation-associated modulation of PSMA may be linked to DNA damage signaling events [42]. Further investigation correlating PSMA trafficking with established DDR markers will be necessary to clarify the underlying mechanism. Despite C4-2 cells are derived from LNCaP cells, they have become androgen-independent [43]. In addition, C4-2 cells are more radioresistant than LNCaP cells by expressing a set of genes associated with cell cycle arrest and DNA repair [27]. Moreover, alternative cell death pathways may contribute to overcoming therapeutic resistance in androgen-independent prostate cancer models. Ferroptosis, an iron-dependent form of regulated cell death characterized by lipid peroxidation and GPX4 inactivation, plays a critical role in prostate cancer progression and treatment response. For instance, modulation of the TfR1/GPX4/ACSL4 axis can trigger the ferroptosis in prostate cancer cells with differential androgen sensitivity (1). Since C4-2 cells exhibit enhanced radioresistance and altered metabolic adaptation compared to LNCaP cells, it is plausible that targeting ferroptosis-related pathways may represent a complementary strategy to improve therapeutic efficacy in androgen-independent models. Whether androgen dependency, DNA repair capacity and ferroptosis of different PCa cells will influence radiation induced expression or migration of PSMA is interesting to be further investigated.

Although C4-2 cells, including C4-2-luc cells have been used for various therapeutic approaches, they were mainly used for subcutaneous xenograft [22,35,44-46]. However, we failed to establish subcutaneous xenograft tumors using C4-2 3R cells. We have also implanted parental C4-2 cells to nude mice through subcutaneous injection, but only one out of five mice could form palpable tumor after 3 months of tracking. This tumor-bearing mouse was intravenous injected with ^{177}Lu-PSMA-617, and the tumor exhibited apparent uptake of this radio-compound as visualized by the single photon emission computed tomography (SPECT)/CT scanning (Supplementary Figure 3). Because C4-2 3R cells showed slower proliferation rate than parental C4-2 cells, it may influence the tumor growth in subcutaneous xenograft model. Nevertheless, the orthotopic tumor model seems unaffected by monitoring the bioluminescent signals. In addition, reporter gene integration and expression may theoretically affect cellular stress or immunogenicity [47]. However, luciferase-tagged human prostate cancer xenografts (e.g., LNCaP-luc) have been successfully established and longitudinally monitored in immunodeficient/nude mouse backgrounds, including subcutaneous settings [48]. Therefore, while host-mediated rejection cannot be excluded, the lack of subcutaneous tumor formation in our C4-2 3R model may also reflect cell intrinsic factors. Evaluation in more profoundly immunodeficient strains (e.g., NSG or NCG mice) warrants future investigation [49].

The primary limitation of this study is the technical difficulty in orthotopic inoculation of cells into prostate by open surgical process. We have inoculated C4-2 3R cells into the prostate glands of 36 nude mice, but only 12 mice successfully formed orthotopic tumors for theranostic monitoring. The failed samples all lost the bioluminescent signals at fourth week after tumor implantation, and no further signals could be detected up to 7 weeks. The successful rate of orthotopic PCa tumor model influences the power of statistical analysis. Therefore, the results should be interpreted as preliminary and exploratory rather than definitive. Future studies with a larger cohort will be required to validate these findings. However, it has provided a convenient method to exclude unsuccessful samples at earlier time for preclinical investigation. Mouse anterior prostate is the largest lobes for easy inoculation of PCa cells for establishment of orthotopic tumor model [50]. Interestingly, the dorsal prostate is androgen sensitive and considered similar with human peripheral zone, while a microscope-guided injection would be necessary for this purpose [31]. In addition to microscope-guided injection, optimization using fine Hamilton syringes, and refinement of surgical procedures, would improve the reproducibility. Importantly, the real-time bioluminescence imaging allows early identification of unsuccessful implantation, thereby enhancing experimental efficiency. C4-2 3R cells would be useful for different orthotopic inoculation techniques to quickly compare the tumor progression om different microenvironments.

 doi:10.20944/preprints202603.2479.v1

In summary, we have used a non-viral *PiggyBac* transposon system to establish a novel PCa cell model that would be useful for multimodality reporter gene imaging. Using bioluminescence imaging as a demonstration, current data suggest that C4-2 3R cells are appropriate for generating orthotopic prostate tumor model that enables convenient and real-time tracking of tumor progression, thereby mitigating the long and unpredictable waiting period associated with the slow-growing nature of prostate cancer cells.

Conclusion

We have established C4-2 3R cells expressing triple reporter genes that could be applied in multimodality molecular imaging of prostate tumor progression in vivo. In the orthotopic model, tumors derived from C4-2 3R cells could be readily monitored non-invasively using bioluminescence imaging, and their growth was more robust than that observed in subcutaneous xenograft tumors. C4-2 3R tumor model also offers a proof-of-concept for quick and real-time evaluation of novel therapeutic strategy, for instance, the combined EBRT and RLT by ^{177}Lu-PSMA-617. Interestingly, ionizing radiation was found to increase the membrane relocation of PSMA in C4-2 cells rather than up-regulation of PSMA gene reported in LNCaP cells. A profound mechanical study would be essential for better understanding the effects of radiation on PSMA expression in androgen-dependent and -independent PCa cells in the future. Taken together, establishment of orthotopic PCa tumor model using C4-2 3R cells provides a dependable framework for preclinical assessment of emerging therapeutic strategies.

Supplementary Materials: The following supporting information can be downloaded at the website of this paper posted on Preprints.org.

Author Contributions: YTC contributed to the concept and the design of the study and manuscript improvement. KXH contributed to data acquisition and analysis. CYW contributed to data interpretation, YJL was responsible for manuscript drafting and data validation. KXH and YJL confirmed the authenticity of all the raw data.

Funding: This project was granted by a bilateral project of Chang-Gung Memorial Hospital, Chang Gung University and National Yang Ming Chiao Tung University (CGMH-NYCU-113-CORPG8P0221), and a grant from National Science and Technology Council (NSTC 114-2314-B-A49 -065 -MY3).

Institutional Review Board Statement: Not applicable.

Informed Consent Statement: Not applicable.

Acknowledgments: The authors acknowledge the" technical services" provided by the National Genomics Center for Clinical and Biotechnological Applications of the Cancer and Immunology Research Center (National Yang Ming Chiao Tung University). The National Core Facility for Biopharmaceuticals (NCFB), National Science and Technology Council (NSTC 114-2740-B-A49-002-) (NSTC 113-2740-B-A49 -002) (NSTC 112-2740-B-A49 -001, NSTC 111-2740-B-A49 -001). The authors also acknowledge the support of Linkou Chang-Gung Memorial Hospital (CGMH) Laboratory Animal Center for PET/CT and SPECT/CT imaging, and the NYCU Instrument Core Facility for supporting the gel imaging system, ELISA reader analyzer, and flow cytometer. Furthermore, we thank the Nuclear Medicine Department of Taipei Veteran General Hospital for providing ^{18}F-PSMA-1007.

Conflicts of Interest: The authors declare that they have no competing interests.

References

1. Rebello, R.J.; Oing, C.; Knudsen, K.E.; Loeb, S.; Johnson, D.C.; Reiter, R.E.; Gillessen, S.; Van der Kwast, T.; Bristow, R.G. Prostate cancer. *Nat Rev Dis Primers* **2021**, *7*, 9, doi:10.1038/s41572-020-00243-0.
2. Horoszewicz, J.S.; Leong, S.S.; Kawinski, E.; Karr, J.P.; Rosenthal, H.; Chu, T.M.; Mirand, E.A.; Murphy, G.P. LNCaP model of human prostatic carcinoma. *Cancer Res* **1983**, *43*, 1809-1818.

 doi:10.20944/preprints202603.2479.v1

3. Shaikh, F.A.; Kurtys, E.; Kubassova, O.; Roettger, D. Reporter gene imaging and its role in imaging-based drug development. *Drug Discov Today* **2020**, *25*, 582-592, doi:10.1016/j.drudis.2019.12.010.
4. Nayerossadat, N.; Maedeh, T.; Ali, P.A. Viral and nonviral delivery systems for gene delivery. *Adv Biomed Res* **2012**, *1*, 27, doi:10.4103/2277-9175.98152.
5. Taghdiri, M.; Mussolino, C. Viral and Non-Viral Systems to Deliver Gene Therapeutics to Clinical Targets. *Int J Mol Sci* **2024**, *25*, doi:10.3390/ijms25137333.
6. Najafi, S.; Rahimpour, A.; Ahmadieh, H.; Rezaei Kanavi, M.; Maleki Tehrani, M.; Suri, F.; Ranjbari, J. The effect of enhancers on the lentiviral transduction efficiency in the human RPE cells: Insights for advancing retinal gene therapies. *Biochem Biophys Rep* **2025**, *42*, 102010, doi:10.1016/j.bbrep.2025.102010.
7. Lin, P.; Correa, D.; Lin, Y.; Caplan, A.I. Polybrene inhibits human mesenchymal stem cell proliferation during lentiviral transduction. *PLoS One* **2011**, *6*, e23891, doi:10.1371/journal.pone.0023891.
8. Mellott, A.J.; Forrest, M.L.; Detamore, M.S. Physical non-viral gene delivery methods for tissue engineering. *Ann Biomed Eng* **2013**, *41*, 446-468, doi:10.1007/s10439-012-0678-1.
9. Wang, K.; Huang, Q.; Qiu, F.; Sui, M. Non-viral Delivery Systems for the Application in p53 Cancer Gene Therapy. *Curr Med Chem* **2015**, *22*, 4118-4136, doi:10.2174/0929867322666151001121601.
10. Aronovich, E.L.; Hyland, K.A.; Hall, B.C.; Bell, J.B.; Olson, E.R.; Rusten, M.U.; Hunter, D.W.; Ellinwood, N.M.; McIvor, R.S.; Hackett, P.B. Prolonged Expression of Secreted Enzymes in Dogs After Liver-Directed Delivery of Sleeping Beauty Transposons: Implications for Non-Viral Gene Therapy of Systemic Disease. *Hum Gene Ther* **2017**, *28*, 551-564, doi:10.1089/hum.2017.004.
11. Claeys Bouuaert, C.; Chalmers, R.M. Gene therapy vectors: the prospects and potentials of the cut-and-paste transposons. *Genetica* **2010**, *138*, 473-484, doi:10.1007/s10709-009-9391-x.
12. Feschotte, C. The piggyBac transposon holds promise for human gene therapy. *Proc Natl Acad Sci U S A* **2006**, *103*, 14981-14982, doi:10.1073/pnas.0607282103.
13. Wilson, M.H.; Coates, C.J.; George, A.L., Jr. PiggyBac transposon-mediated gene transfer in human cells. *Mol Ther* **2007**, *15*, 139-145, doi:10.1038/sj.mt.6300028.
14. Chen, Y.L.; Wang, S.Y.; Liu, R.S.; Wang, H.E.; Chen, J.C.; Chiou, S.H.; Chang, C.A.; Lin, L.T.; Tan, D.T.; Lee, Y.J. Remnant living cells that escape cell loss in late-stage tumors exhibit cancer stem cell-like characteristics. *Cell Death Dis* **2012**, *3*, e399, doi:10.1038/cddis.2012.136.
15. Lin, M.Y.; Wang, C.Y.; Chan, Y.H.; Su, S.P.; Chiang, H.K.; Yang, M.H.; Lee, Y.J. The Emergence of Tumor-Initiating Cells in an Advanced Hypopharyngeal Tumor Model Exhibits Enhanced Angiogenesis and Nuclear Factor Erythroid 2-Related Factor 2-Associated Antioxidant Effects. *Antioxid Redox Signal* **2024**, *41*, 505-521, doi:10.1089/ars.2023.0310.
16. Sartor, O.; de Bono, J.; Chi, K.N.; Fizazi, K.; Herrmann, K.; Rahbar, K.; Tagawa, S.T.; Nordquist, L.T.; Vaishampayan, N.; El-Haddad, G.; et al. Lutetium-177-PSMA-617 for Metastatic Castration-Resistant Prostate Cancer. *N Engl J Med* **2021**, *385*, 1091-1103, doi:10.1056/NEJMoa2107322.
17. Algin, E.; Okudan, B.; Acikgoz, Y.; Sayan, H.; Bal, O.; Seven, B. Impact of 68Ga-PSMA PET/CT on Survival and Management in Prostate Cancer. *Curr Med Imaging* **2024**, *20*, e15734056276494, doi:10.2174/0115734056276494231207101146.
18. Teunissen, F.R.; Oprea-Lager, D.E.; Peters, S.M.B.; Smeenk, R.J.; Heskamp, S.; Bussink, J. Current Developments in Combining External-Beam Radiotherapy and (177)Lu-Labeled PSMA Ligands for Prostate Cancer Treatment. *J Nucl Med* **2025**, doi:10.2967/jnumed.125.270465.
19. Arbuznikova, D.; Klotsotyra, A.; Uhlmann, L.; Domogalla, L.C.; Steinacker, N.; Mix, M.; Niedermann, G.; Spohn, S.K.B.; Freitag, M.T.; Grosu, A.L.; et al. Exploring the role of combined external beam radiotherapy and targeted radioligand therapy with [(177)Lu]Lu-PSMA-617 for prostate cancer - from bench to bedside. *Theranostics* **2024**, *14*, 2560-2572, doi:10.7150/thno.93249.
20. Kleinendorst, S.C.; Oosterwijk, E.; Bussink, J.; Westdorp, H.; Konijnenberg, M.W.; Heskamp, S. Combining Targeted Radionuclide Therapy and Immune Checkpoint Inhibition for Cancer Treatment. *Clin Cancer Res* **2022**, *28*, 3652-3657, doi:10.1158/1078-0432.CCR-21-4332.
21. Ruigrok, E.A.M.; van Vliet, N.; Dalm, S.U.; de Blois, E.; van Gent, D.C.; Haeck, J.; de Ridder, C.; Stuurman, D.; Konijnenberg, M.W.; van Weerden, W.M.; et al. Extensive preclinical evaluation of lutetium-177-labeled

 doi:10.20944/preprints202603.2479.v1

PSMA-specific tracers for prostate cancer radionuclide therapy. *Eur J Nucl Med Mol Imaging* **2021**, *48*, 1339-1350, doi:10.1007/s00259-020-05057-6.

22. Meyer, C.; Stuparu, A.; Lueckerath, K.; Calais, J.; Czernin, J.; Slavik, R.; Dahlbom, M. Tandem Isotope Therapy with (225)Ac- and (177)Lu-PSMA-617 in a Murine Model of Prostate Cancer. *J Nucl Med* **2023**, *64*, 1772-1778, doi:10.2967/jnumed.123.265433.
23. Kristiansson, A.; Orbom, A.; Ahlstedt, J.; Karlsson, H.; Zedan, W.; Gram, M.; Akerstrom, B.; Strand, S.E.; Altai, M.; Strand, J.; et al. (177)Lu-PSMA-617 Therapy in Mice, with or without the Antioxidant alpha(1)-Microglobulin (A1M), Including Kidney Damage Assessment Using (99m)Tc-MAG3 Imaging. *Biomolecules* **2021**, *11*, doi:10.3390/biom11020263.
24. Chen, Y.-L.; Wang, Y.-C.; Hou, K.-Y.; Lin, M.-Y.; Lin, Y.-C.; Chuang, H.-Y.; Lee, Y.-J. Use of piggyBac Transposon System Constructed Murine Breast Cancer Model for Reporter Gene Imaging and Characterization of Metastatic Tumor Cells. *Journal of Medical and Biological Engineering* **2022**, *42*, 341-350, doi:10.1007/s40846-022-00703-w.
25. Kang, Y.; Zhang, X.Y.; Jiang, W.; Wu, C.Q.; Chen, C.M.; Gu, J.R.; Zheng, Y.F.; Xu, C.J. The piggyBac transposon is an integrating non-viral gene transfer vector that enhances the efficiency of GDEPT. *Cell Biol Int* **2009**, *33*, 509-515, doi:10.1016/j.cellbi.2009.01.017.
26. Pavese, J.; Ogden, I.M.; Bergan, R.C. An orthotopic murine model of human prostate cancer metastasis. *J Vis Exp* **2013**, e50873, doi:10.3791/50873.
27. Xie, B.X.; Zhang, H.; Yu, L.; Wang, J.; Pang, B.; Wu, R.Q.; Qian, X.L.; Li, S.H.; Shi, Q.G.; Wang, L.L.; et al. The radiation response of androgen-refractory prostate cancer cell line C4-2 derived from androgen-sensitive cell line LNCaP. *Asian J Androl* **2010**, *12*, 405-414, doi:10.1038/aja.2009.91.
28. Lim, D.J.; Liu, X.L.; Sutkowski, D.M.; Braun, E.J.; Lee, C.; Kozlowski, J.M. Growth of an androgen-sensitive human prostate cancer cell line, LNCaP, in nude mice. *Prostate* **1993**, *22*, 109-118, doi:10.1002/pros.2990220203.
29. Jennbacken, K.; Gustavsson, H.; Tesan, T.; Horn, M.; Vallbo, C.; Welen, K.; Damber, J.E. The prostatic environment suppresses growth of androgen-independent prostate cancer xenografts: an effect influenced by testosterone. *Prostate* **2009**, *69*, 1164-1175, doi:10.1002/pros.20965.
30. Saar, M.; Korbel, C.; Linxweiler, J.; Jung, V.; Kamradt, J.; Hasenfus, A.; Stockle, M.; Unteregger, G.; Menger, M.D. Orthotopic tumorgrafts in nude mice: A new method to study human prostate cancer. *Prostate* **2015**, *75*, 1526-1537, doi:10.1002/pros.23027.
31. Liu, W.; Zhu, Y.; Ye, L.; Zhu, Y.; Wang, Y. Establishment of an orthotopic prostate cancer xenograft mouse model using microscope-guided orthotopic injection of LNCaP cells into the dorsal lobe of the mouse prostate. *BMC Cancer* **2022**, *22*, 173, doi:10.1186/s12885-022-09266-0.
32. Baba, D.; Çoban, S.; Çalışkan, A.; Senoglu, Y.; Kayıkçı, M.; Tekin, A. Optimizing Prostate Cancer Diagnosis: A Prospective, Randomized Comparison of 12-core vs. 20-core Biopsy for Detection Accuracy and Upgrading Risk. *Journal of Urological Surgery* **2025**, doi:10.4274/jus.galenos.2025.2025-2-9.
33. Yamamichi, F.; Matsuoka, T.; Shigemura, K.; Kawabata, M.; Shirakawa, T.; Fujisawa, M. Potential establishment of lung metastatic xenograft model of androgen receptor-positive and androgen-independent prostate cancer (C4-2B). *Urology* **2012**, *80*, 951 e951-957, doi:10.1016/j.urology.2012.06.023.
34. Li, M.; Wang, Y.; Liu, M.; Lan, X. Multimodality reporter gene imaging: Construction strategies and application. *Theranostics* **2018**, *8*, 2954-2973, doi:10.7150/thno.24108.
35. Stuparu, A.D.; Meyer, C.A.L.; Evans-Axelsson, S.L.; Luckerath, K.; Wei, L.H.; Kim, W.; Poddar, S.; Mona, C.E.; Dahlbom, M.; Girgis, M.D.; et al. Targeted alpha therapy in a systemic mouse model of prostate cancer - a feasibility study. *Theranostics* **2020**, *10*, 2612-2620, doi:10.7150/thno.42228.
36. Han, M.; Yu, D.; Song, Q.; Wang, J.; Dong, P.; He, J. Polybrene: Observations on cochlear hair cell necrosis and minimal lentiviral transduction of cochlear hair cells. *Neurosci Lett* **2015**, *600*, 164-170, doi:10.1016/j.neulet.2015.06.011.
37. Inada, E.; Saitoh, I.; Watanabe, S.; Aoki, R.; Miura, H.; Ohtsuka, M.; Murakami, T.; Sawami, T.; Yamasaki, Y.; Sato, M. PiggyBac transposon-mediated gene delivery efficiently generates stable transfectants derived from cultured primary human deciduous tooth dental pulp cells (HDDPCs) and HDDPC-derived iPS cells. *Int J Oral Sci* **2015**, *7*, 144-154, doi:10.1038/ijos.2015.18.

 doi:10.20944/preprints202603.2479.v1

38. Ali, F.Z. Prostate Cancer Imaging Beyond PSMA: Applications of GRPR, AR, and Amino Acid Tracers. *Diagnostics (Basel)* **2025**, *15*, doi:10.3390/diagnostics15212737.
39. Sheehan, B.; Neeb, A.; Buroni, L.; Paschalis, A.; Riisnaes, R.; Gurel, B.; Gil, V.; Miranda, S.; Crespo, M.; Guo, C.; et al. Prostate-Specific Membrane Antigen Expression and Response to DNA Damaging Agents in Prostate Cancer. *Clin Cancer Res* **2022**, *28*, 3104-3115, doi:10.1158/1078-0432.CCR-21-4531.
40. Zhang, C.; Liu, J.; Wu, J.; Ranjan, K.; Cui, X.; Wang, X.; Zhang, D.; Zhu, S. Key molecular DNA damage responses of human cells to radiation. *Front Cell Dev Biol* **2024**, *12*, 1422520, doi:10.3389/fcell.2024.1422520.
41. Mahaney, B.L.; Meek, K.; Lees-Miller, S.P. Repair of ionizing radiation-induced DNA double-strand breaks by non-homologous end-joining. *Biochem J* **2009**, *417*, 639-650, doi:10.1042/bj20080413.
42. Bakht, M.K.; Beltran, H. Biological determinants of PSMA expression, regulation and heterogeneity in prostate cancer. *Nat Rev Urol* **2025**, *22*, 26-45, doi:10.1038/s41585-024-00900-z.
43. Chen, Q.; Watson, J.T.; Marengo, S.R.; Decker, K.S.; Coleman, I.; Nelson, P.S.; Sikes, R.A. Gene expression in the LNCaP human prostate cancer progression model: progression associated expression in vitro corresponds to expression changes associated with prostate cancer progression in vivo. *Cancer Lett* **2006**, *244*, 274-288, doi:10.1016/j.canlet.2005.12.027.
44. Mamouni, K.; Zhang, S.; Li, X.; Chen, Y.; Yang, Y.; Kim, J.; Bartlett, M.G.; Coleman, I.M.; Nelson, P.S.; Kucuk, O.; et al. A Novel Flavonoid Composition Targets Androgen Receptor Signaling and Inhibits Prostate Cancer Growth in Preclinical Models. *Neoplasia* **2018**, *20*, 789-799, doi:10.1016/j.neo.2018.06.003.
45. Johnson, T.J.; Hoti, N.; Liu, C.; Chowdhury, W.H.; Li, Y.; Zhang, Y.; Lupold, S.E.; Deweese, T.; Rodriguez, R. Bicalutamide-activated oncolytic adenovirus for the adjuvant therapy of high-risk prostate cancer. *Cancer Gene Ther* **2013**, *20*, 394-402, doi:10.1038/cgt.2013.34.
46. Chen, Y.; Gera, L.; Zhang, S.; Li, X.; Yang, Y.; Mamouni, K.; Wu, A.Y.; Liu, H.; Kucuk, O.; Wu, D. Small molecule BKM1972 inhibits human prostate cancer growth and overcomes docetaxel resistance in intraosseous models. *Cancer Lett* **2019**, *446*, 62-72, doi:10.1016/j.canlet.2019.01.010.
47. Podetz-Pedersen, K.M.; Vezys, V.; Somia, N.V.; Russell, S.J.; McIvor, R.S. Cellular immune response against firefly luciferase after sleeping beauty-mediated gene transfer in vivo. *Hum Gene Ther* **2014**, *25*, 955-965, doi:10.1089/hum.2014.048.
48. Zou, M.; Jiao, J.; Zou, Q.; Xu, Y.; Cheng, M.; Xu, J.; Zhang, Y. Multiple metastases in a novel LNCaP model of human prostate cancer. *Oncol Rep* **2013**, *30*, 615-622, doi:10.3892/or.2013.2305.
49. Smutova, V.; Para, C.; Foret, M.K.; Bennamoune, N.; Hung, S.; Spickler, C.; Riffon, R.; Rowe, J.; Festin, S.; Authier, S. Non-Clinical Cell Therapy Development Using the NCG Mouse Model as a Test System. *Int J Toxicol* **2023**, *42*, 232-253, doi:10.1177/10915818221150790.
50. Ahmat Amin, M.K.B.; Shimizu, A.; Zankov, D.P.; Sato, A.; Kurita, S.; Ito, M.; Maeda, T.; Yoshida, T.; Sakaue, T.; Higashiyama, S.; et al. Epithelial membrane protein 1 promotes tumor metastasis by enhancing cell migration via copine-III and Rac1. *Oncogene* **2018**, *37*, 5416-5434, doi:10.1038/s41388-018-0286-0.